Plasma assisted dry reforming of methanol for clean syngas production and high-efficiency CO_2 conversion

Hao Zhang[a,b], Xiaodong Li[b,*], Fengsen Zhu[b], Kefa Cen[b], Changming Du[c] and Xin Tu[d,*]

[a] *Institute of Energy and Power Engineering, Zhejiang University of Technology, Hangzhou, 310014, China*

[b] *State Key Laboratory of Clean Energy Utilization, Zhejiang University, Hangzhou 310027, China*

[c] *School of Environmental Science and Engineering, Sun Yat-sen University, Guangzhou 510275, China*

[d] *Department of Electrical Engineering and Electronics, University of Liverpool, Liverpool L69 3GJ, UK*

Abstract

Herein, the CO_2 reforming of methanol, or can be called dry reforming of methanol (DRM), was investigated for the first time using a rotating gliding arc plasma. The effect of input CH_3OH concentration on the reaction performance of the DRM process has been investigated. Optical emission spectroscopy (OES) has been used to give insights into the formation of reactive species in the plasma chemical reactions. In addition, the possible reaction mechanisms of the plasma DRM process have been discussed. The plasma assisted DRM has been demonstrated to be a promising route for clean syngas production and high-efficiency CO_2 conversion. This process provided a significantly higher efficiency for CO_2 conversion compared to other plasma technologies, while maintaining a CO_2 flow rate (or processing capacity) of one or several orders of magnitude higher.

Keywords: Rotating gliding arc (RGA); Dry reforming of methanol; Syngas production; CO_2 conversion

1. Introduction

Currently, the need to develop renewable and alternative energy sources and radically reduce greenhouse gas emissions is becoming ever more urgent. Therefore, increasing attention worldwide has been paid to the development of new and efficient methods of simultaneous production of syngas and reduction of greenhouse gases, such as dry methane reforming process [1-3]. Nevertheless, technical problems with the handling, storage, and transport of gas fuels largely restrict its

* *Corresponding authors.* Tel.: +86 571 87952037 (X. D. Li), +44-1517944513 (X. Tu).
E-mail addresses: lixd@zju.edu.cn (X. D. Li), xin.tu@liverpool.ac.uk (X. Tu)

widespread use, particularly in mobile systems (*e.g.*, on-board vehicles) [4, 5].

On-board methanol reforming has been considered as a promising portable syngas production technology due to a couple of advantages over other potential fuels: unlike gasoline or diesel fuel, methanol can be readily produced from biomass; it is easily adaptable to the current infrastructure; it is easily transported and stored; it has nearly nil sulphur content, and finally it has a high hydrogen density [6-9]. Methanol conversion via steam reforming (H_2O + CH_3OH) [6, 7, 9], methanol decomposition (pure CH_3OH or noble gas + CH_3OH) [10, 11], partial oxidation (O_2/Air + CH_3OH) [4], and oxidation steam reforming (H_2O + O_2/Air + CH_3OH) [5, 8] has been extensively investigated. Whereas, CO_2 reforming of methanol, or can be called dry reforming (CO_2 + CH_3OH) of methanol (DRM), has not been reported yet. This process should be of particular interest because it can simultaneously convert the main greenhouse gas CO_2 into the value-added CO and produce H_2. The DRM process has a good application foreground particularly in vehicles because it can convert the CO_2 in the exhaust into CO and simultaneously produce syngas as a supplementary fuel for the internal combustion engines which has been shown to significantly improve the engine performance and reduce pollutant emission (*e.g.*, CO and NO_x) [12, 13]. Note that vehicle emission has been considered as one of the primary sources for CO_2, particularly in developed countries [14].

Compared to traditional catalytic reforming process that has problems of high capital costs, requirement of high temperature, large equipment size, and rapid loss of catalyst activity [15, 16], non-thermal plasma technology provides a more attractive route for portable methanol reforming at low temperatures. In non-thermal plasmas, the overall gas temperature can be as low as room temperature, while the electrons are highly energetic with a typical electron temperature of 1-10 eV (10^4-10^5K), which is sufficient to break down most chemical bonds of molecules and produce highly reactive species for the initiation and propagation of chemical reactions. High reaction rate and fast attainment of steady state in plasma processes allows rapid start-up and shutdown of the process compared to catalytic processes, which is more suitable for on-board applications [1, 2, 17].

Herein, the DRM process was studied for the first time using a novel rotating gliding arc (RGA) plasma co-driven by a magnetic field and tangential flow, aiming at clean syngas production and CO_2 conversion in one step. Quite different from the traditional flat gliding arc that consists of two divergent knife-shaped electrodes [18], the RGA reactor provides a more stable plasma reaction zone by generating a rapidly rotating arc (80-120 rotations per second) under the synergistic effect of swirling flow and Lorentz force, in which the retention time of reactants can be significantly

increased [19]. The formed “plasma disc” area is shown in Fig. 1. Detailed descriptions of this reactor are available in our previous work [19, 20].

2. Experimental

The experimental setup mainly consists of a RGA reactor, a mass flow controller (MFC), a syringe pump, temperature controllers, a DC power supply, a two-stage condenser system and measurement systems. It is schematically shown in Fig. 1. Methanol was controlled and injected into the gas tube by a high-resolution syringe pump (Harvard, 11 plus), and the mixture of CO_2 and methanol was then heated to 100 °C in a stainless steel tubing with an inner diameter of 4 mm (40 cm in length) to generate a steady-state vapour before flowing into the RGA reactor. The RGA reactor was powered by a DC 10kV power source for the generating and maintaining of plasma. A 40-kΩ resistance was connected in series in the circuit for current limitation and stabilization. A two-stage condenser was added after the reactor to remove and collect the condensable vapors in the effluent stream: a first-stage coil condenser equipped with an ice-cooled water circulation system and a second-stage liquid trap that placed inside an ice water container.

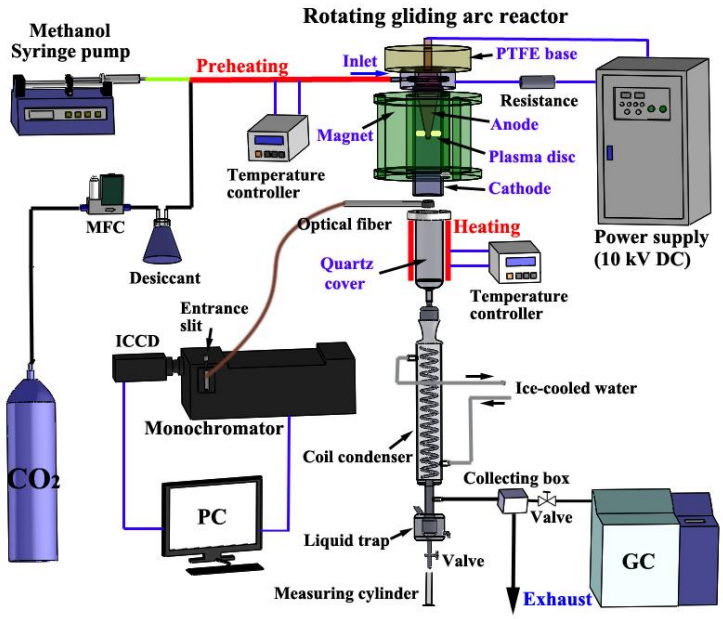

Fig. 1. Schematic diagram of the RGA plasma assisted DRM system

The gaseous products were measured by a gas chromatograph (GC) (GC9790A, Fuli Analytical Instrument) equipped with a thermal conductivity detector (TCD) for detecting H_2 and O_2 as well as

a flame ionization detector (FID) for detecting CO, CO_2, and CH_4. No C_2 or higher hydrocarbons were detected in the effluent gas. The GC columns are 5A molecular sieve packed column (2m×3 mm, helium carrier gas) for the TCD detector and GDX-104 packed column (2m×3 mm, helium carrier gas) for the FID detector. The FID detector is equipped with catalytic methanation to analyze CO and CO_2. The optical emission spectroscopy (OES) system comprises a 750-mm monochromator (PI-Acton 2750), an intensified charge-coupled device (ICCD) (PI-MAX 2, 512×512 pixel), and an optical fiber. The optical fiber was placed at around 10 cm above the "plasma disc" to collect the plasma radiation.

The performance of the DRM process was evaluated in terms of conversions of CH_3OH (X_{CH3OH}), CO_2 (X_{CO2}), and total-carbon (X_{TC}), selectivity of gas product, energy conversion efficiency of the reaction, as well as the efficiency for CO_2 conversion (the definitions of these parameters are available in the Electronic Supporting Information).

3. Results and discussion

Fig. 2 and Fig. 3 show the effect of input CH_3OH concentration on the performance of the DRM process. The total flow rate was fixed at 0.6 mol/min. H_2 and CO were detected as the main gas products, while trace amount of CH_4 and O_2 (<3.4% selectivity for each) were also formed.

In our previous study, for pure CO_2 decomposition process in the RGA plasma (flow rate = 11.5 L/min), the conversion of CO_2 was only 1%. Whereas, as shown in Fig. 2, the addition of 5% (mol/mol) CH_3OH into CO_2 significantly enhanced the CO_2 conversion to 3.9%, indicating that CH_3OH facilitates the conversion of CO_2. With further increasing CH_3OH concentration to 35% (mol/mol), the CO_2 conversion escalated to 18.6%. Strong OH spectral bands were observed in the CH_3OH/CO_2 spectra and the H_2/CO ratio was lower than 1.0, demonstrating the occurrence of reverse water-gas shift (RWGS) reaction (Eq. (1)) in the DRM process.

$$CO_2 + H_2 \rightarrow H_2O\ (g) + CO \qquad \Delta H^o = 41.2\ kJ/mol \tag{1}$$

The facilitating effect of CH_3OH on CO_2 conversion arises from the RWGS reaction as well as the oxidation reactions between H_2 (or CO) and O_2 that produced from CO_2 decomposition. On the other side, CO_2 can also promote the dissociation of CH_3OH in the same way. The decrease of CO_2 concentration from 95 to 80% led to a significant drop of CH_3OH conversion from 64.4 to 29.9 %.

It is somewhat surprising that a drastic lift of CH_3OH conversion from 29.9 to 50.9% appeared when the CH_3OH concentration further raised from 20 to 25%. Simultaneously, the significant rise of specific energy input also manifested the enhancement of CH_3OH decomposition reaction (endothermic) in the plasma system. The noticeable elevation of CH_3OH conversion was probably attributed to the rise of electron temperature (known from optical emission diagnostics), impelling the decomposition reaction of CH_3OH. Then, with further increase of CH_3OH concentration, the CH_3OH conversion continued to decline. The total-carbon conversion first increased to a maximum of 24.6% at a CH_3OH concentration of 25% and then slightly decreased.

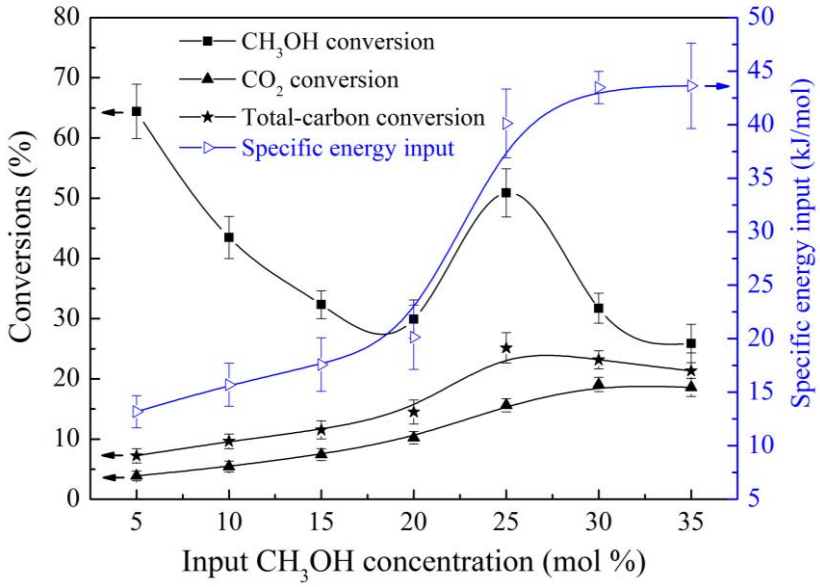

Fig. 2. Effect of CH_3OH concentration on conversions of CH_3OH, CO_2, and total-carbon, as well as specific energy input

The strong RWGS reaction during the DRM process was responsible for the higher selectivity of CO than H_2, as shown in Fig. 3. With the decrease of CO_2 concentration, the RWGS reaction was thought to be gradually weakened, giving rise to an increase in both H_2 selectivity and H_2/CO ratio. The H_2 selectivity increased from 5.1 to 39.3 % and the H_2/CO ratio escalated linearly from 0.18 to 0.73 with rising CH_3OH concentration from 5 to 35%. The production rate of H_2O was also estimated based on the hydrogen balance of the DRM process. After adding the estimated H_2O production rate into the calculation, the final oxygen balance was 92.9-99.0% under the tested conditions. The selectivity of converted CH_3OH towards H_2O was found to decrease drastically from 93.0 to 57.9% with increasing CH_3OH concentration from 5 to 35%, revealing less and less

proportion of produced H_2 took part in the RWGS reaction. The selectivity of CO also showed an increase with rising CH_3OH concentration, probably resulted from the reduce of O_2 molecules in the system that can deplete CO molecules.

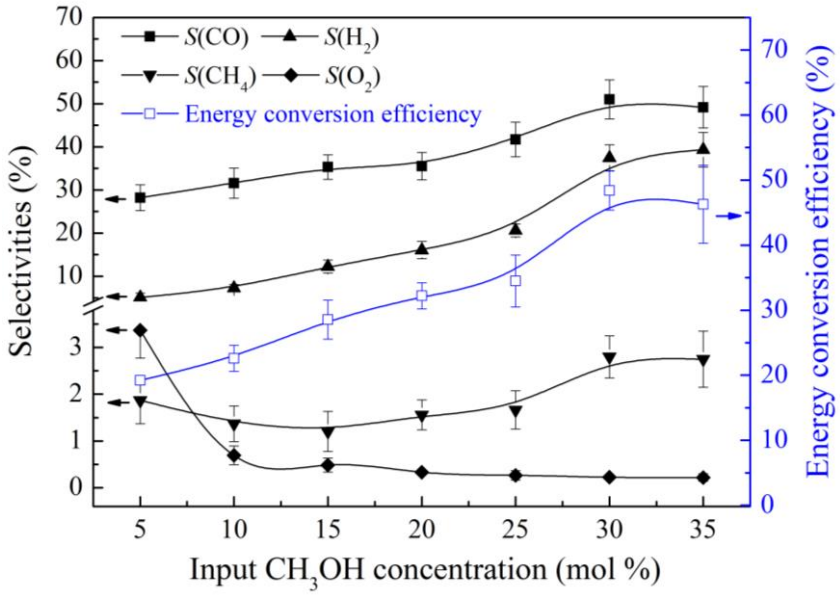

Fig. 3. Effect of CH_3OH concentration on product selectivity and energy conversion efficiency

The selectivities towards CH_4 and O_2 were only 1.2 to 2.8% and 0.2 to 3.4%, respectively. The increasing production rate of H_2 and CO with the increase of CH_3OH concentration should be responsible for both the increase of CH_4 selectivity and decrease of O_2 selectivity due to the methanation reactions of CO [21] and oxidation reactions of H_2 and CO. The energy conversion efficiency (ECE) significantly increased with increasing CH_3OH concentration due to the weakening of the RWGS reaction that could consume H_2 molecules. The maximum ECE reached up to 49.3% at a CH_3OH concentration of 30% and the slight drop of ECE at CH_3OH concentration = 35% may be resulted from the instability of the arc operation.

It should be noted that a few scholars [22] also defined the energy efficiency as the ratio of the total energy of the product to the input plasma energy in plasma assisted fuel reforming process. Based on this definition, the energy efficiency of the DRM process increased from 49.3 to 116.2% with increasing CH_3OH concentration from 5 to 35% and then dropped to 107.8% when the CH_3OH concentration reached 35%.

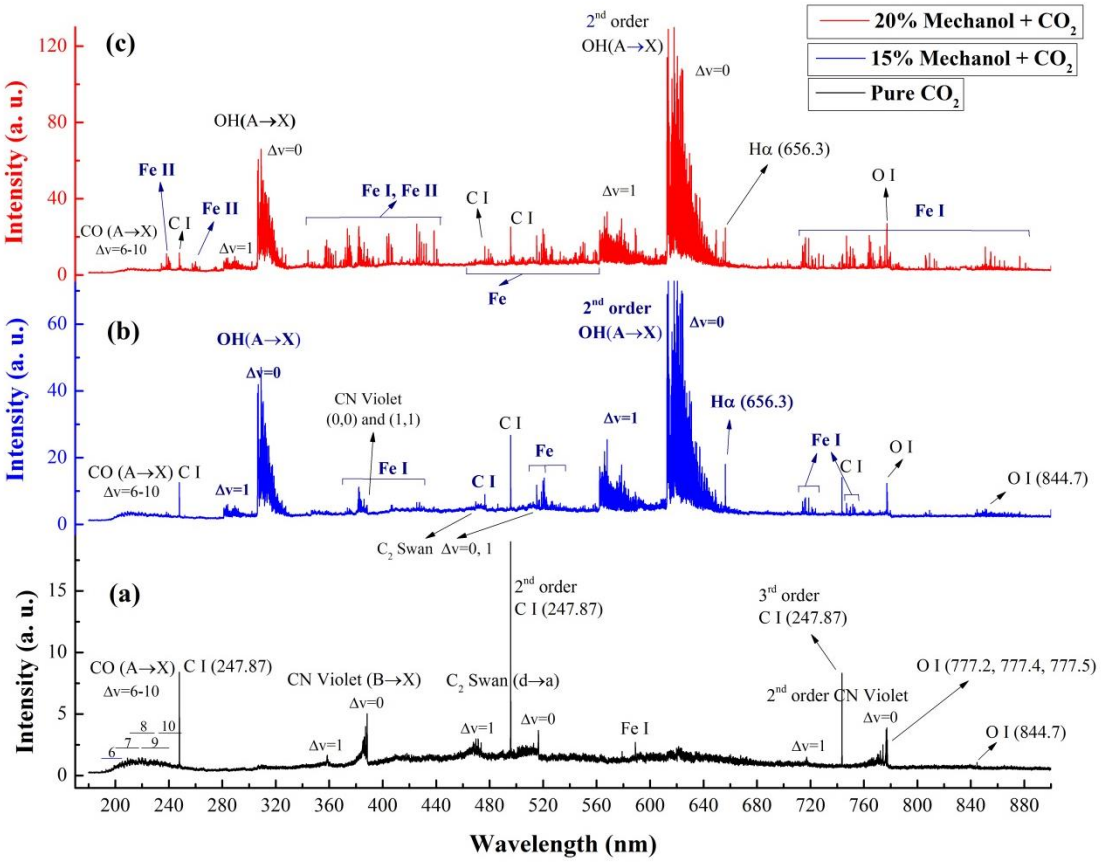

Fig. 4. Emission spectra of (a) pure CO_2, (b) 15% CH_3OH/CO_2, and (c) 20% CH_3OH/CO_2 plasmas (Q = 0.6 mol/min)

To give insight into the mechanisms of the DRM process, the reactive species formed in the process were detected using a spectrometer. Typical emission spectra of pure CO_2, 15% CH_3OH/CO_2, and 20% CH_3OH/CO_2 plasmas are shown in Fig. 4. For the pure CO_2 spectra, the CO, C, CN, C_2, and O species, as well as several Fe lines were observed. Whereas, strong OH bands and Hα spectral line also occurred in the CH_3OH/CO_2 spectra, indicating that the addition of CH_3OH into CO_2 gave rise to the formation of H_2O and H_2 molecules. According to the Fe and Hα spectral lines, we also estimated the electron temperature Te and electron density Ne, which could greatly influence the reaction performance in plasma (the calculation methods are available in the Electronic Supporting Information). The Te of Fe increased from 7830 ± 400 to 8450 ± 420 K and the Ne reduced from 7.4 ± 1.0 to 3.8 ± 1.2 $\times 10^{14}$ cm^{-3} with increasing CH_3OH concentration from 5 to 35 %. It is worth noting that the Ne in the RGA plasmas is significantly higher than typical non-thermal plasmas, such as dielectric barrier discharges (DBD) (10^{10}-10^{13} cm^{-3}) and corona discharges (10^{9}-10^{13} cm^{-3}) [17, 23], indicating a higher processing capacity of the RGA plasmas.

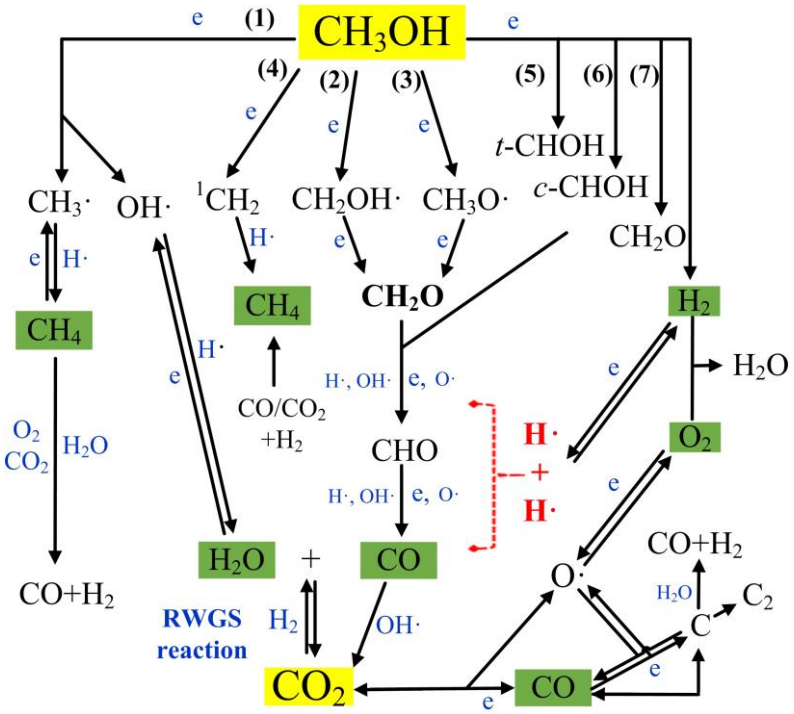

Fig. 5. Schematic representation of the mechanisms of the RGA assisted DRM process ("e" on the paths denotes "electron")

The possible prominent chemical paths in the RGA assisted DRM process are schematically shown in Fig. 5. The complex reactions in the plasma bulk are initiated from the dissociation of CH_3OH and CO_2 molecules that resulted from the frequent impact of energetic electrons. The overall CH_3OH decomposition reaction is as follows.

$$CH_3OH \rightarrow 2H_2 + CO \qquad \Delta H_{298K}=128.1\ kJ/mol \qquad (2)$$

According to previous studies, there are primarily seven initial reaction paths for methanol dissociation [24-26], which are labelled as (1)-(7) in Fig. 5. Paths (1)-(3) directly produce $CH_3\cdot$ + $OH\cdot$, $CH_2OH\cdot$ + $H\cdot$ and $CH_3O\cdot$ + $H\cdot$, respectively. The other four paths have transition states. In path (4), one of the H atoms in the $CH_3\cdot$ group migrates to the $OH\cdot$ group to form a van der Waals (vdw) complex and then produce $^1CH_2$ + H_2O [24, 27]. Paths (5) and (6) correspond to the H_2 elimination from the $CH_3\cdot$ group to form *tran*- and *cis*-CHOH. In path (7), the elimination of H_2 forms CH_2O and H_2 via a four-member ring transition state [27].

To investigate the roles that different paths played in the dissociation of methanol, we also collected the spectra of CH_3OH/N_2 and CH_3OH/Ar plasmas with the absence of CO_2, in which CH_3OH primarily underwent the decomposition process. In the CH_3OH/N_2 and CH_3OH/Ar plasmas,

only quite weak OH spectral lines could be observed, indicating that paths (1) and (4) seem to be negligible, because OH radicals can easily form via the two paths. Another phenomenon that can support this conclusion is that only a CH_4 selectivity of 1.2 to 2.8% and no C_2H_4 were obtained in the DRM process, considering that paths (1) and (4) produce CH_3 and CH_2 radicals that can then readily generate CH_4 and C_2H_4 molecules respectively via the hydrogenation reactions [28]. Actually, the small amount of CH_4 was more likely to form from the methanation reactions of CO_2, CO and/or C [21].

Paths (2) and (3) are also considered to play little role in the dissociation of methanol because they are even less energetically favoured in comparison to paths (1) and (4) due to the higher dissociation energies [24]. Therefore, the H_2 elimination routes (paths (5)-(7)) with lower activation energies than the abovementioned paths should predominate in the dissociation of methanol [24, 27], largely contributing to the production of H_2 molecules simultaneously.

The formed *tran*-CHOH, *cis*-CHOH and CH_2O are the key intermediate products of the process, which are very unstable in non-thermal plasmas and would then readily dissociate to produce the main products: H_2 and CO.

No O spectral line or O_2 product was detected in the methanol decomposition process both in N_2 and Ar due to the high bond dissociation energy of H_2C-O, HC-O and CO (7.7, 8.4, 11.1 eV). Therefore, the electron impact dissociation of CH_2O should proceed via the following paths.

$$CH_2O + e \rightarrow CHO\cdot + H\cdot + e \quad (3)$$

$$CHO\cdot + e \rightarrow CO\cdot + H\cdot + e \quad (4)$$

$$H\cdot + H\cdot \rightarrow H_2 \quad (5)$$

The O·, H·, and OH· that present in the plasma bulk may also take part in the conversion of CH_2O and/or CHO, generating CO, CO_2, H·, and H_2 etc. [29].

The H_2/CO ratios of the DRM process were only 0.18-0.73% under the studied conditions, which is much lower than the stoichiometric ratio of methanol decomposition reaction (H_2/CO = 2.0). In addition, compared to the methanol decomposition process in N_2 in the RGA plasmas, the H_2 yields as well as the H_2/CO ratios of the DRM process are much lower while the CO yields are significantly higher (as shown in Table S2 in the Electronic Supporting Information). Therefore, the low H_2 and high CO production rate as well as the strong OH spectral lines in the CH_3OH/CO_2 spectra clearly demonstrate the occurrence of the RWGS reaction (Eq. (1)) in the DRM process.

Due to the abundance of CO_2 molecules in the plasma bulk, the RWGS reaction probably plays an important role in the DRM process, resulting in an increase in the selectivity to CO but decrease in the selectivity to H_2. The RWGS reaction can also largely contribute to the conversion of CO_2 to CO.

In addition to the RWGS reaction, CO_2 molecules can also decompose from the direct electron impact dissociation of CO_2 via Eq. (6) [30], giving rise to the production of CO and O (and then O_2) simultaneously. Whereas, the direct electron impact route was thought to play less of role in CO_2 conversion, because only a CO_2 conversion rate of around 1% could be obtained in the pure CO_2 decomposition process in the RGA plasma.

$$CO_2 + e \rightarrow CO + O\cdot + e \quad (6)$$

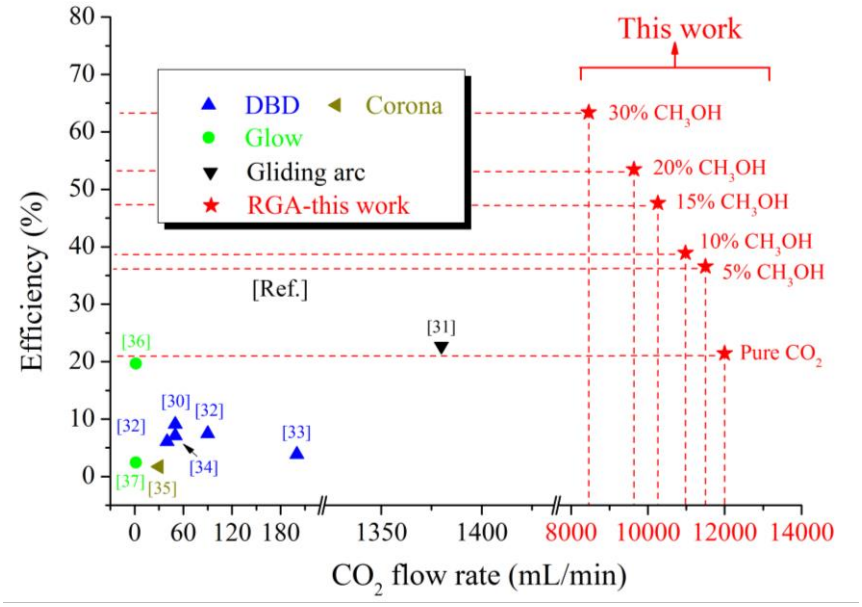

Fig. 6. Comparison of the efficiency for CO_2 conversion using different non-thermal plasma technologies

Compared with other non-thermal assisted methanol conversion technologies (shown in Table S3 in the Electronic Supporting Information), the RGA assisted DRM process shows a moderate CH_3OH conversion, a high CO selectivity, but a relatively low H_2 selectivity. It is interesting to note that the RGA assisted DRM process can be used to generate much cleaner gas products of which syngas is the main one with a high production rate. When compared with other non-thermal plasma assisted CO_2 decomposition technologies, as shown in Fig. 6 (and Table S4 in the Electronic

Supporting Information), the RGA assisted DRM process shows significant advantages in terms of feed flow rate (i.e., processing capacity), CO_2 conversion and efficiency for CO_2 conversion. The efficiency in this study could reach up to 34.0-62.4%, which is much higher than that of other plasma technologies (0.95-19.33%) [30-38], such as DBD [30, 32-34], corona [35], glow discharge [36-38] and flat gliding arc [31], while maintaining a processing capacity of one or several order of magnitude higher. The addition of 5% CH_3OH into pure CO_2 could give rise to a significant lift of efficiency for CO_2 conversion from around 18.0% to 34.0% in the RGA system.

4. Conclusions

In conclusion, this communication reported a new method of plasma assisted dry reforming of methanol (DRM) process, which was demonstrated to be a promising route for portable clean syngas production and high-efficiency CO_2 conversion. The reverse water-gas shift (RWGS) reaction and oxidation reaction of CO and H_2 in the process facilitate the conversion of both CH_3OH and CO_2. This process can produce clean syngas with high capacity and simultaneously, the efficiency for CO_2 conversion was significantly improved compared to other non-thermal plasma technologies. In addition, the RGA plasma enhanced the processing capacity of the existing non-thermal plasmas by one or several order of magnitude, which should be more suitable for further applications.

Electronic Supporting Information available: Definition of parameters, Observed spectral lines in the optical emission spectra; Calculation methods of electron excitation temperature and electron density; Comparison of the DRM and methanol decomposition processes; Comparison with other non-thermal technologies for methanol conversion and CO_2 decomposition.

Acknowledgments

This work is supported by the National Natural Science Foundation of China (51576174), the Specialized Research Fund for the Doctoral Program of Higher Education of China (20120101110099) and the Fundamental Research Funds for the Central Universities (2015FZA4011).

References:

[1] X. Tu, J.C. Whitehead, Plasma-catalytic dry reforming of methane in an atmospheric dielectric barrier

discharge: Understanding the synergistic effect at low temperature. Appl. Catal., B 125 (2012) 439-448.

[2] R. Snoeckx, R. Aerts, X. Tu, A. Bogaerts, Plasma-based dry reforming: a computational study ranging from the nanoseconds to seconds time scale. J. Phys. Chem. C 117 (2013) 4957-4970.

[3] S.Y. Liu, D.H. Mei, Z. Shen, X. Tu, Nonoxidative conversion of methane in a dielectric barrier discharge reactor: Prediction of reaction performance based on neural network model. J. Phys. Chem. C 118 (2014) 10686-10693.

[4] L. Mo, X. Zheng, C. Yeh, Selective production of hydrogen from partial oxidation of methanol over silver catalysts at low temperatures. Chem. Commun. 12 (2004) 1426-1427.

[5] C. Li, R. Lin, H. Lin, Y. Lin, Y. Lin, C. Chang, L. Chen, K. Chen, Catalytic performance of plate-type Cu/Fe nanocomposites on ZnO nanorods for oxidative steam reforming of methanol. Chem. Commun. 47 (2011) 1473-1475.

[6] I. Uriz, G. Arzamendi, P.M. Diéguez, F.J. Echave, O. Sanz, M. Montes, L.M. Gandía, CFD analysis of the effects of the flow distribution and heat losses on the steam reforming of methanol in catalytic (Pd/ZnO) microreactors. Chem. Eng. J. 238 (2014) 37-44.

[7] O.P. Klenov, L.L. Makarshin, A.G. Gribovskiy, D.V. Andreev, V.N. Parmon, CFD modeling of compact methanol reformer. Chem. Eng. J. 282 (2015) 91-100.

[8] G. Avgouropoulos, J. Papavasiliou, T. Ioannides, Hydrogen production from methanol over combustion-synthesized noble metal/ceria catalysts. Chem. Eng. J. 154 (2009) 274-280.

[9] A.G. Gribovskiy, L.L. Makarshin, D.V. Andreev, O.P. Klenov, V.N. Parmon, Thermally autonomous microchannel reactor to produce hydrogen in steam reforming of methanol. Chem. Eng. J. 273 (2015) 130-137.

[10] Q. Gao, C. Zhang, S. Wang, W. Shen, Y. Zhang, H. Xu, Y. Tang, Preparation of supported Mo2C-based catalysts from organic–inorganic hybrid precursor for hydrogen production from methanol decomposition. Chem. Commun.46 (2010) 6494-6496.

[11] H. Zhang, X.D. Li, F.S. Zhu, Z. Bo, K.F. Cen, X. Tu, Non-oxidative decomposition of methanol into hydrogen in a rotating gliding arc plasma reactor. Int. J. Hydrogen Energ. 2015, 40(46), 15901-15912.

[12] Chao, Y., Lee, H., Chen, S. and Chang, M. Onboard motorcycle plasma-assisted catalysis system–Role of plasma and operating strategy. Int. J. Hydrogen Energ. 34 (2009) 6271-6279.

[13] M.A.S. Al-Baghdadi, Performance study of a four-stroke spark ignition engine working with both of hydrogen and ethyl alcohol as supplementary fuel. Int. J. Hydrogen Energ. 25 (2000) 1005-1009.

[14] G. Pinto, M.T. Oliver-Hoyo, Using the relationship between vehicle fuel consumption and CO_2 emissions to illustrate chemical principles. J. Chem. Educ. 85 (2008) 218.

[15] S. Sá, H. Silva, L. Brandão, J.M. Sousa, A. Mendes, Catalysts for methanol steam reforming–A review. Appl. Catal., B 99 (2010) 43-57.

[16] H. Junge, B. Loges, M. Beller, Novel improved ruthenium catalysts for the generation of hydrogen from alcohols. Chem. Commun. 5 (2007) 522-524.

[17] X. Tu, J.C. Whitehead, Plasma dry reforming of methane in an atmospheric pressure AC gliding arc discharge: Co-generation of syngas and carbon nanomaterials. Int. J. Hydrogen Energ. 39 (2014) 9658-9669.

[18] A. Fridman, S. Nester, L.A. Kennedy, A. Saveliev, O. Mutaf-Yardimci, Gliding arc gas discharge. Prog. Energy Combust. Sci. 25 (1998) 211-231.

[19] H. Zhang, X.D. Li, Y.Q. Zhang, T. Chen, J.H. Yan, C.M. Du, Rotating gliding arc codriven by magnetic field and tangential flow. IEEE Trans. Plasma Sci. 40 (2012) 3493-3498.

[20] H. Zhang, C.M. Du, A.J. Wu, Z. Bo, J.H. Yan, X.D. Li. Rotating gliding arc assisted methane decomposition in nitrogen for hydrogen production. Int. J. Hydrogen Energ. 39 (2014) 12620-12635.

[21] F. Bustamante, R.M. Enick, A.V. Cugini, R.P. Killmeyer, B.H. Howard, K.S. Rothenberger, M.V. Ciocco, B.D. Morreale, S. Chattopadhyay, S. Shi, High-temperature kinetics of the homogeneous reverse water-gas

shift reaction. AICHe J. 50 (2004) 1028-1041

[22] S. Kado, Y. Sekine, T. Nozaki, and K. Okazaki. Diagnosis of atmospheric pressure low temperature plasma and application to high efficient methane conversion. Catal. Today 89 (2004) 47-55.

[23] X. Tu, B. Verheyde, S. Corthals, S. Paulussen, B.F. Sels, Effect of packing solid material on characteristics of helium dielectric barrier discharge at atmospheric pressure. Phys. Plasmas 18 (2011) 80702.

[24] Y. Han, J. Wang, D. Cheng, C. Liu, Density functional theory study of methanol conversion via cold plasmas. Ind. Eng. Chem. Res. 45 (2006) 3460-3467.

[25] A. Chang, S.H. Lin, A theoretical study of the O (1D)+ CH_4 reaction I. Chem. Phys. Lett. 363 (2002) 175-181.

[26] R. De Avillez Pereira, D.L. Baulch, M.J. Pilling, S.H. Robertson, G. Zeng, Temperature and pressure dependence of the multichannel rate coefficients for the CH_3+ OH system. J. Phys. Chem. A 101 (1997) 9681-9693.

[27] W.S. Xia, R.S. Zhu, M.C. Lin, A.M. Mebel, Low-energy paths for the unimolecular decomposition of CH_3OH: A G2M/statistical theory study. Faraday Discuss. 119 (2002) 191-205.

[28] T. Sreethawong, P. Thakonpatthanakun, S. Chavadej, Partial oxidation of methane with air for synthesis gas production in a multistage gliding arc discharge system. Int. J. Hydrogen Energ. 32 (2007) 1067-1079.

[29] C. Liu, R. Mallinson, L. Lobban, Nonoxidative methane conversion to acetylene over zeolite in a low temperature plasma. J. Catal. 179 (1998) 326-334.

[30] R. Aerts, W. Somers, A. Bogaerts, Carbon dioxide splitting in a dielectric barrier discharge plasma: A combined experimental and computational study. ChemSusChem 8 (2015) 702-716.

[31] A. Indarto, D.R. Yang, J. Choi, H. Lee, and H.K. Song. Gliding arc plasma processing of CO_2 conversion. J. Hazard. Mater. 146 (2007) 309-315.

[32] Q. Yu, M. Kong, T. Liu, J. Fei, and X. Zheng. Characteristics of the decomposition of CO_2 in a dielectric packed-bed plasma reactor. Plasma Chem. Plasma P. 32 (2012) 153-163.

[33] S. Paulussen, B. Verheyde, X. Tu, C. De Bie, T. Martens, D. Petrovic, A. Bogaerts, and B. Sels. Conversion of carbon dioxide to value-added chemicals in atmospheric pressure dielectric barrier discharges. Plasma Sources Sci. T. 19 (2010) 34015.

[34] D.H. Mei, X.B. Zhu, Y.L. He, J.D. Yan, and X. Tu. Plasma-assisted conversion of CO_2 in a dielectric barrier discharge reactor: understanding the effect of packing materials. Plasma Sources Sci. T. 24 (2014) 15011.

[35] W. Xu, M. Li, G. Xu, and Y. Tian. Decomposition of CO_2 using DC corona discharge at atmospheric pressure. Jpn. J. Appl. Phys. 43 (2004) 8310.

[36[J. Wang, G. Xia, A. Huang, S.L. Suib, Y. Hayashi, and H. Matsumoto. CO_2 decomposition using glow discharge plasmas. J. Catal. 185 (1999) 152-159.

[37] S.L. Brock, T. Shimojo, M. Marquez, C. Marun, S.L. Suib, H. Matsumoto, and Y. Hayashi. Factors influencing the decomposition of CO_2 in AC fan-type plasma reactors: Frequency, waveform, and concentration effects. J. Catal. 184 (1999) 123-133.

[38] S.L. Brock, M. Marquez, S.L. Suib, Y. Hayashi, and H. Matsumoto. Plasma decomposition of CO_2 in the presence of metal catalysts. J. Catal. 180 (1998) 225-233.